

Computational analysis of the human HSPH/HSPA/DNAJ family and cloning of a human HSPH/HSPA/DNAJ expression library

Jurre Hageman · Harm H. Kampinga

Received: 23 April 2008 / Revised: 19 June 2008 / Accepted: 19 June 2008 / Published online: 7 August 2008
© Cell Stress Society International 2008

Abstract In this manuscript, we describe the generation of a gene library for the expression of HSP110/HSPH, HSP70/HSPA and HSP40/DNAJ members. First, the heat shock protein (HSP) genes were collected from the gene databases and the gene families were analyzed for expression patterns, heat inducibility, subcellular localization, and protein homology using several bioinformatics approaches. These results can be used as a working draft model until data are confirmed by experimental approaches. In addition, we describe the generation of a HSPA/DNAJ overexpression library and tested the effect of different fusion tags on HSPA and DNAJ members using different techniques for measuring chaperone activity. These results show that we have cloned a high-quality heat shock protein expression library containing most members from the HSPH, HSPA, DNAJA and DNAJB families which will be useful for the chaperone community to unravel the function of the highly diverse family of human molecular chaperones.

Keywords HspH · HspA · DnaJ · Hsp110 · Hsp70 · Hsp40 · Human chaperones · Bio-informatics

Introduction

All organisms, except some hyperthermophilic archaea, contain the family of HSP110/HSPH, HSP70/HSPA, and HSP40/DNAJ chaperones (Gribaldo et al. 1999). HSPA and DNAJ proteins function as molecular chaperones to assist in processes such as translation and transport of proteins across membranes.

The HSPA machine consists of the core HSPA protein along with a transient array of different co-factors such as DNAJ, HSPH, BAG-1, Hip, CHIP, and HSPBP1 (Kampinga 2006). The HSPH/HSPA and DNAJ families are protein families consisting of many members and as a whole, the HSPH/HSPA/DNAJ gene family is the largest chaperone gene family found in humans.

It is thought that many of its members are specialized (Sahi and Craig 2007). For instance, members of the HSPA, DNAJ, and HSPH family exist that are only expressed under stress conditions suggesting that these are specialized to function in the proteotoxic stress response (Albanese et al. 2006). Constitutively expressed members are found as well and such members are found in several cellular compartments such as the cytosol, mitochondria and the endoplasmic reticulum (ER) suggesting that cellular compartmentalization has driven some of the HSPA/DNAJ gene expansion (Broccchieri et al. 2008). In addition, some members have only been found at specific developmental stages or in specific cell types indicating the need for specialized members for specific substrates expressed only during specific developmental stages or in certain specialized cell types.

In contrast to the gene expansion as a result of compartmentalization, the gene expansion as a result of cellular specialization or organism development is poorly understood. It has been suggested that HSPA and DNAJ proteins bind small hydrophobic regions (Rudiger et al. 1997; Rudiger et al.

J. Hageman
Section of Radiation and Stress Cell Biology,
Department of Cell Biology,
University Medical Center Groningen, University of Groningen,
Groningen, The Netherlands

H. H. Kampinga (✉)
Ant. Deusinglaan 1,
9713 AV, Groningen, The Netherlands
e-mail: h.h.kampinga@med.umcg.nl

2001); yet there is great diversity and multiplicity within these families of which most members have not yet been studied in detail.

Although the various chaperone genes are now relatively well annotated, the molecular function for most of its members is currently unknown. For each of the families, only a single or restricted number of proteins has been studied in detail. In this paper, we used bioinformatics approaches to study the different HSPH, HSPA, and DNAJ members (Broccieri et al. 2007). Thereafter, we describe the construction of a human HSPH/HSPA/DNAJ expression library.

Materials and methods

Bioinformatics

HSP gene retrieval HSPH, HSPA and DNAJ genes were collected from National Center for Biotechnology Information (NCBI) Gene (Maglott et al. 2007). Mouse orthologs were identified using NCBI Homologene (Wheeler et al. 2007). Protein molecular weights were calculated using the clone manager 7 suite (Sci-Ed Software).

EST count analysis Expression data based on tissue-specific and developmental stage specific expressed sequence tag (EST) numbers were collected from the NCBI UniGene database (Wheeler et al. 2007). EST numbers are displayed as counts per million.

Affymetrix gene array Investigation of genome-wide heat-induced transcriptional activation was described previously (Page et al. 2006). These experiments were performed in HeLa cells using a 1.5-h heat shock at 43°C. Recovery times were 0.5, 2, and 4 h at 37°C. Affymetrix gene array data were downloaded (Page et al. 2006) and linear induction was calculated from the 2log fold change. Affymetrix uses different annotations for its probe sets. *_at* suffix designates a unique probe set, whereas the *_s_at* and *_x_at* suffixes designate probe sets that can cross hybridize with multiple genes. In the case of redundant probe sets, *_at* suffix were selected by default. In the case of no available *_at* suffix, the first probe set was selected routinely.

Subcellular localization analysis Predictions on subcellular localizations were performed using pSort, pTarget, CELLO, Multiloc, and Proteome analyst (Szafron et al. 2004; Yu et al. 2006; Guda 2006; Hoglund et al. 2006; Horton et al. 2007). Sequences from complete gene families were uploaded as fasta files. In each case, only the first rank localization is displayed. For all predictors, the default settings for mammalian or animal proteins were used. The

presence of prenelation motifs was determined using the PrePS webserver (Maurer-Stroh et al. 2007).

Protein Alignments Primary amino acid alignments were performed in ClustalX2 using the neighbor-joining algorithm and Blosum matrixes at the default settings (Larkin et al. 2007). Bootstrap analysis was performed using 1,000 random number generator seeds and 1,000 bootstrap trials. Phylograms were made by importing the homology tree output of ClustalX in TreeView (Page 1996). The distance is depicted in the scale bar of Fig. 1 as 0.1 amino acids substitutions per position.

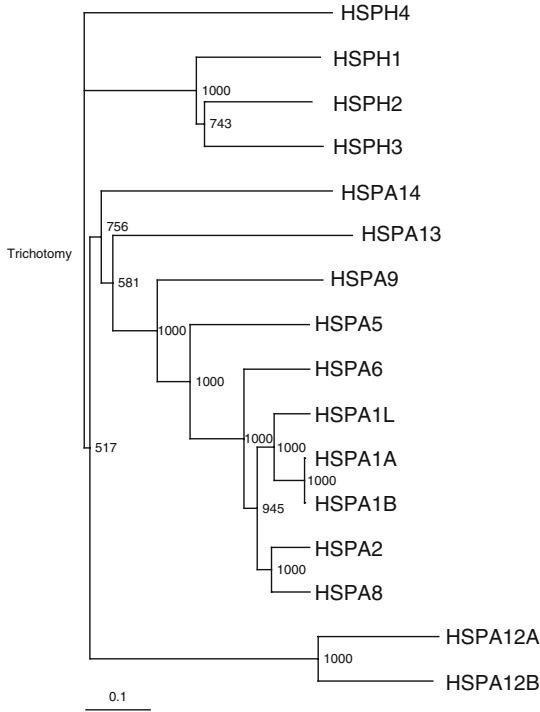
Library cloning and validation

Gene Cloning

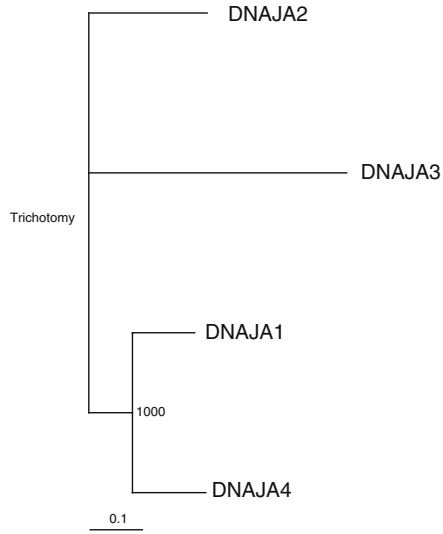
Detailed information about the plasmids used in this study can be found in Fig. 2. Briefly, tetracycline-inducible HSP expression plasmids were constructed as follows. First, the green fluorescent protein (GFP) and the v5 tag, harboring a Kozak consensus ATG initiation codon and lacking a stop codon, were cloned in the pCDNA5 FLP recombination target (FRT)/TO vector (Invitrogen). Subsequently, the coding sequence of the different chaperones was amplified using the primers listed in supplemental Table 8. As a template source, complementary DNA (cDNA) was made from total RNA as previously described (Hageman et al. 2005). As a source of total RNA, QPCR Human reference Total RNA (Stratagene) was used, which is a mixed source of RNA from the following cell line derivations: adenocarcinoma, mammary gland; hepatoblastoma, liver; adenocarcinoma, cervix; embryonal carcinoma, testis; glioblastoma, brain; melanoma, skin; liposarcoma, histiocytic lymphoma, macrophage, histocyte; lymphoblastic leukemia, T lymphoblast; plasmacytoma, myeloma, B lymphocyte. DNAJB4, DNAJB5, and DNAJB8 were amplified from cloned full-length cDNAs purchased from Open Biosystems (clone ID: DNAJB4: 4340658, DNAJB5: 4684829, and DNAJB8: 5296554). The fragments were cloned in pCDNA5 fit to GFP lacking a stop codon resulting in a N-GFP-cDNA-C protein. The presence of the correct gene was sequence verified. Protein expression was verified by Western blotting. Subsequently, fragments were subcloned to pCDNA5 fit to v5 and pCDNA5 fit to.

Fig. 1 Phylograms for the HSPH/A (A), DNAJA (B), DNAJB (C), and DNAJC (D) families. Primary amino acid alignments were performed using the Neighbor-joining algorithm using a Blosum scoring matrix in ClustalX (see “Methods” for details). Bootstrap values are indicated on the branch-points

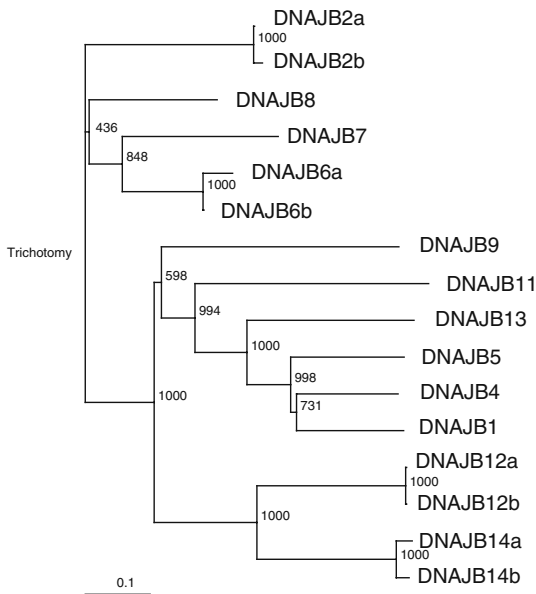
A HSPA AND HSPH



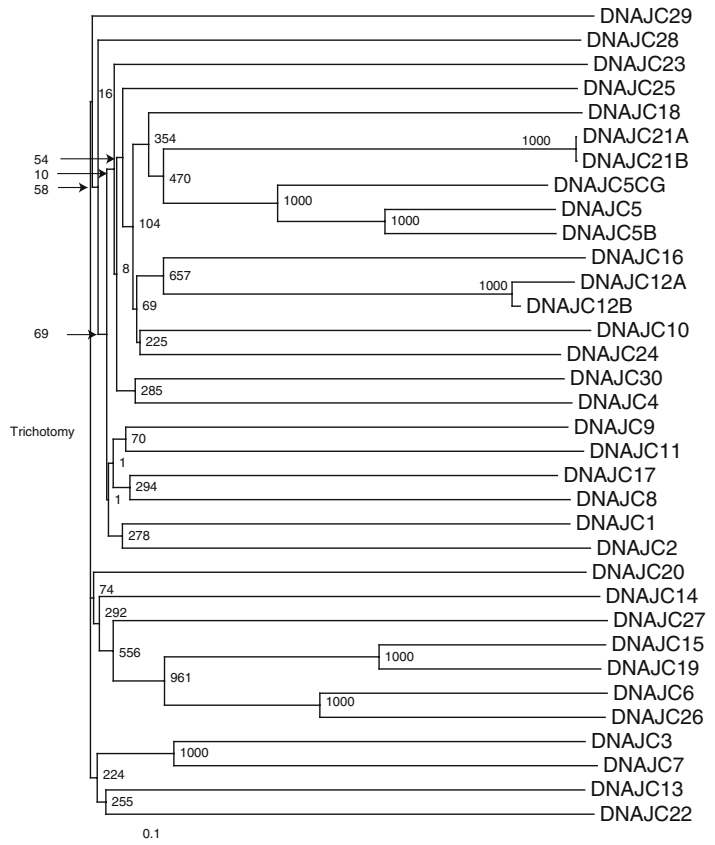
B DNAJA



C DNAJB



D DNAJC



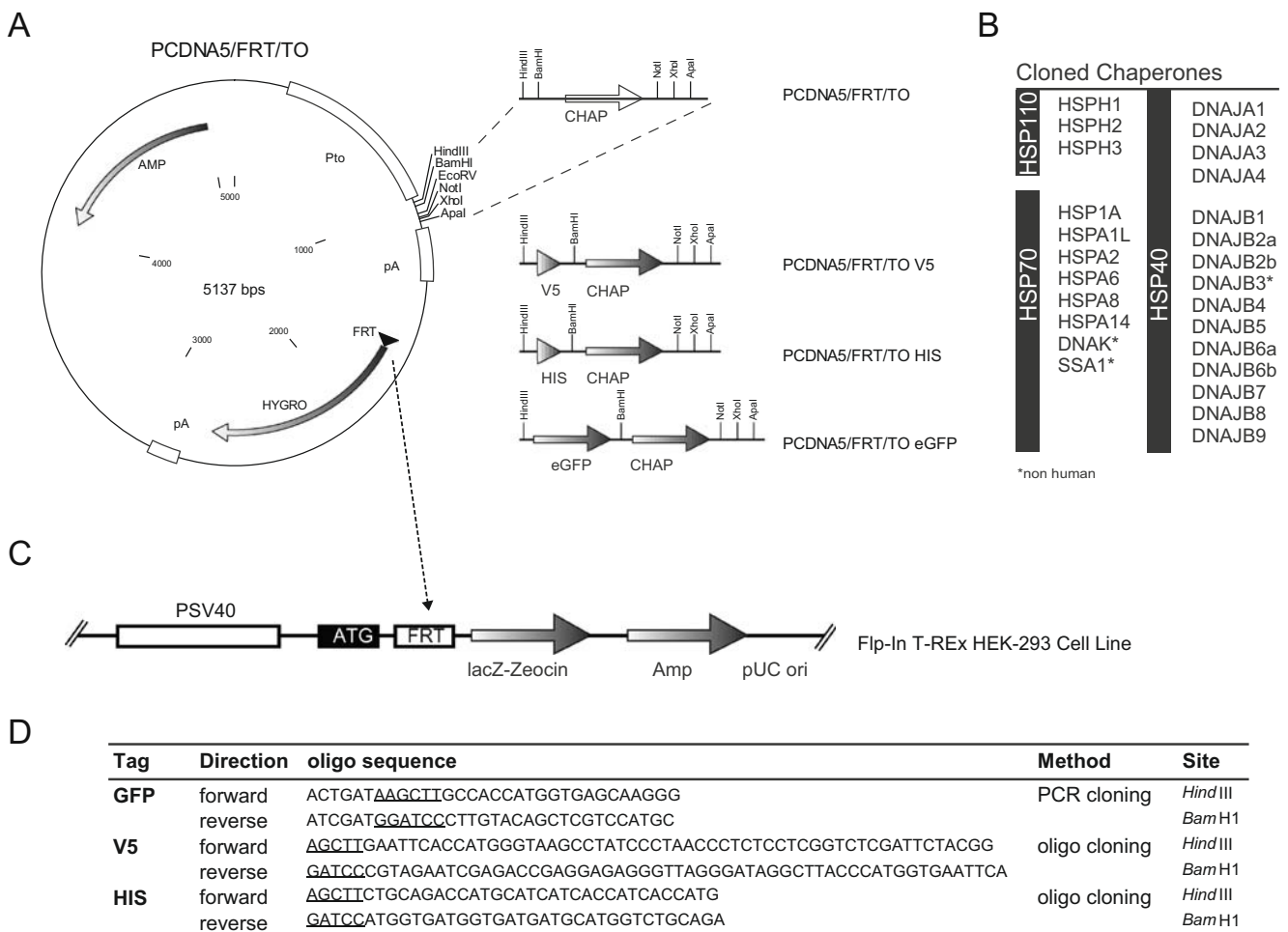


Fig. 2 Schematic overview of the library construction. (A) The pCDNA5/FRT/TO vector system together with the cloned fusion tags. (B) List of the cloned molecular chaperones. (C) Schematic

representation of the FRT locus within the Flp-In T-REx HEK-293 cell line. (D) Primer sequences for the construction of the indicated fusion tags

Luciferase refolding Assay Cell lysis and luciferase activity measurements were done as previously described (Michels et al. 1995). Luciferase activity was plotted relative to the percentage of activity in an unheated control. Error bars on plots represent standard deviations.

Filter trap assay To determine protein aggregates, the filter trap assay was performed as previously described (Carra et al. 2005). Briefly, 10, 2, and 0.4 μ g of protein extracts were applied onto 0.2- μ m pore cellulose acetate membrane pre-washed with FTA + 0.1% sodium dodecyl sulfate (SDS). Mild suction was applied and the membrane was washed three times. Aggregated proteins trapped in the membrane were probed with a mouse anti-GFP antibody JL-8 (Clontech) at a 1:5,000 dilution or a mouse anti-V5 antibody (Invitrogen) at a 1:5,000 dilution followed by horseradish peroxidase (HRP)-conjugated anti-mouse secondary antibody (Amersham) at 1:5,000 dilution. Visualisation was

performed using enhanced chemiluminescence and Hyperfilm (ECL, Amersham).

Results

Bioinformatic analysis on the HSPH, HSPA, and DNAJ gene family

Collecting the HSPH, HSPA, and DNAJ gene family

In order to get a comprehensive overview of the gene family, we first extracted all human HSPH, HSPA, and DNAJ family members from the NCBI gene database. It should be noted that beside these protein encoding genes, we found many pseudogenes scattered throughout the human genome. Typically, pseudogenes show types of

Table 1 Overview of the human HSP70/HSP40 gene family

	Gene Name	Protein Name	Alternative Name	Human GeneID	Mouse ortholog ID	Locus (human)	Protein length (aa)	Calculated Mass (kD)
HSPH	HSPH1	HSPH1	HSP105	10808	15505	13q12.3	858	96.9
	HSPH2	HSPA4	HSPA4, APG-2; HSP110	3308	15525	5q31.1–q31.2	840	94.3
	HSPH3	HSPA4L	HSPA4L, APG-1	22824	18415	4q28	839	94.5
	HSPH4	HSPH4	HYOU1; GRP170	10525	12282	11q23.1	999	111.3
HSPA	HSPA1A	HSPA1A	HSP70–1, HSP72, HSPA1	3303	193740	6p21.3	641	70.0
	HSPA1B	HSPA1B	HSP70–2	3304	15511	6p21.3	641	70.0
	HSPA1L	HSPA1L	hum70t, hum70t	3305	15482	6p21.3	641	70.4
	HSPA2	HSPA2	Heat-shock 70kD protein-2	3306	15512	14q24.1	639	70.0
	HSPA5	HSPA5	BIP, GRP78, MIF2	3309	14828	9q33–q34.1	654	71.0
	HSPA6	HSPA6	heat shock 70kD protein 6 (HSP70B')	3310	X	1q23	643	71.0
	HSPA7	HSPA7		3311	X	1q23.3	?	?
	HSPA8	HSPA8	HSC70, HSC71, HSP71, HSP73	3312	15481	11q24.1	646/493	70.9/53.5
	HSPA9	HSPA9	GRP75, HSPA9B, MOT, MOT2, PBP74, mot-2	3313	15526	5q31.1	679	73.7
	HSPA12A	HSPA12A	FLJ13874, KIAA0417	259217	73442	10q26.12	1296	141.0
	HSPA12B	HSPA12B	RP23–32L15.1, 2700081N06Rik	116835	72630	20p13	686	75.7
	HSPA13	HSPA13	Stch	6782	110920	21q11	471	51.9
	HSPA14	HSPA14	HSP70–4, HSP70L1, MGC131990	51182	50497	10p14	509	54.8
	DNAJA	DNAJA1	DNAJA1	DJ-2; DjA1; HDJ2; HSDJ; HSJ2; HSPF4; hDJ-2	3301	15502	9p13–p12	397
DNAJA2		DNAJA2	DNJ3; mDj3; DNAJ3; HIRIP4	10294	56445	16q11.1–q11.2	412	45.7
DNAJA3		DNAJA3	Tid-1; Tid11	9093	83945	16p13.3	480	52.5
DNAJA4		DNAJA4	Dj4; Hsj4	55466	58233	15q24.1	397	44.7
DNAJB	DNAJB1	DNAJB1	HSPF1; HSP40	3337	81489	19p13.2	340	38.2
	DNAJB2	DNAJB2	HSJ1; HSPF3; DNAJB10	3300	56812	2q32–q34	324/277	35,6/30,6
	DNAJB3	DNAJB3	Hsj3; Msj1; MSJ-1	414061	15504	1 D (Mm)	242	26.7
	DNAJB4	DNAJB4	Hsc40	11080	67035	1p31.1	337	37.8
	DNAJB5	DNAJB5	Hsc40; HSP40-3	25822	56323	9p13.2	348/241	39,1/26,9
	DNAJB6	DNAJB6	Mrj; mDj4	10049	23950	7q36.3	326/241	36.1
	DNAJB7	DNAJB7	Dj5; mDj5	150353	57755	22q13.2	309	35.4
	DNAJB8	DNAJB8	mDj6	165721	56691	3q21.3	232	25.7
	DNAJB9	DNAJB9	Mdg1; mDj7; ERdj4	4189	27362	7q31	223	25.5
	DNAJB11	DNAJB11	Dj9; ABBP-2; ERdj3	51726	67838	3q28	358	40.5
DNAJB12	DNAJB12	Dj10; mDj10	54788	56709	10q22.2	375	41.9	
DNAJB13	DNAJB13	Tsarg	374407	69387	11q13.4	316	36.1	
DNAJB14	DNAJB14	EGNR9427; FLJ14281	79982	70604	4q23	379/294	42,5/33,5	
DNAJC	DNAJC1	DNAJC1	MTJ1; ERdj1; ERj1p; DNAJ11	64215	13418	0p12.33–p12.32	554	63.9
	DNAJC2	DNAJC2	Zrf1; Zrf2; MIDA1	27000	22791	7q22	621	72.0
	DNAJC3	DNAJC3	p58; mp58; Prkri; DNAJc3; p58IPK; DNAJc3b	5611	100037258	13q32	504	57.6
	DNAJC4	DNAJC4	HSPf2; Mcg18	3338	57431	11q13	135	15.2
	DNAJC5	DNAJC5	Csp	80331	13002	20q13.33	198	22.1
	DNAJC5B	DNAJC5B	CSP-beta	85479	66326	8q12.3	199	22.5
	DNAJC5G	DNAJC5G	MGC107182	285126	231098	2p23.3	189	21.4
	DNAJC6	DNAJC6	mKIAA0473	9829	72685	1pter-q31.3	913	100.0
	DNAJC7	DNAJC7	Ttc2; mDj11; mTpr2	7266	56354	17q11.2	484	55.5
DNAJC8	DNAJC8	AL024084; AU019262	22826	68598	1p35.2	264	31.0	
DNAJC9	DNAJC9	AU020082	23234	108671	10q22.3	260	29.9	

Table 1 (continued)

Gene Name	Protein Name	Alternative Name	Human GeneID	Mouse ortholog ID	Locus (human)	Protein length (aa)	Calculated Mass (kD)
DNAJC10	DNAJC10	JPDI; ERdj5	54431	66861	2q32.1	793	91.1
DNAJC11	DNAJC11	FLJ10737	55735	230935	1p36.23	559	63.3
DNAJC12	DNAJC12	Jdp1; mJDP1	56521	30045	10q22.1	198/107	23,4/12,5
DNAJC13	DNAJC13	Rme8; RME-8; Gm1124	23317	235567	3q22.1	2243	254.4
DNAJC14	DNAJC14	HDJ3; LIP6; DRIP78	85406	74330	12q13.13	702	78.6
DNAJC15	DNAJC15	DNAJd1	29103	66148	13q14.1	150	16.4
DNAJC16	DNAJC16	mKIAA0962	23341	214063	1p36.1	782	90.6
DNAJC17	DNAJC17	C87112	55192	69408	15q15.1	304	34.7
DNAJC18	DNAJC18	MGC29463	202052	76594	5q31.2	358	41.5
DNAJC19	DNAJC19	TIM14; TIMM14	131118	67713	3q26.33	116	12.5
DNAJC20	DNAJC20	JAC1; HSC20	150274	100900	22q12.1	235	27.4
DNAJC21	DNAJC21	GS3; JJJ1; DNAJA5;	134218	78244	5p13.2	576/531	67,1/62,0
DNAJC22	DNAJC22	FLJ13236; Wurst	79962	72778	12q13.12	341	38.1
DNAJC23	DNAJC23	Sec63; AI649014	11231	140740	6q21	760	88.0
DNAJC24	DNAJC24	<i>DPH4</i> ; zinc finger, CSL-type containing 3	120526	99349	11p13	149	17.1
DNAJC25	DNAJC25	<i>ba16L21.2.1</i> ; DnaJ-like protein	548645	X	9q31.3	360	42.4
DNAJC26	DNAJC26	<i>GAK</i> ; cyclin G associated kinase	2580	231580	4p16	1311	143.2
DNAJC27	DNAJC27	<i>RBJ</i> ; Rabj	51277	217378	2p23.3	273	30.9
DNAJC28	DNAJC28	<i>Orf28 open reading frame 28</i> ; C21orf55	54943	246738	1q25	454	51.1
DNAJC29	DNAJC29	<i>SACS</i> ; <i>Sacsin</i>	26278	50720	13q12	4432	504.6
DNAJC30	DNAJC30	<i>WBSCR18</i>	84277	66114	7q11.23	226	26.0

decay such as frame-shifts, stop-codons or gaps. For the HSPA family alone, already 30 pseudogenes have been documented (Broccieri et al. 2008). For gene selection, we extracted the annotated non-pseudo genes from the NCBI gene bank (Maglott et al. 2007). We found 4 HSPH chaperones, 13 HSPA chaperones, and 49 DNAJ chaperones. The genes including the protein name, the old and alternative names, the NCBI human gene ID, the mouse ortholog gene ID, the human gene locus, the protein length, and the calculated molecular mass are listed in Table 1. Classically, human chaperones were ranked according to molecular mass. However, as can be seen from Table 1, many HSP genes deviate from this and contain only a HSP-like domain such as the HSP70 ATPase domain or the HSP40 DNAJ domain. For instance, while many HSP40/DNAJ proteins are around 40 kD, the sizes of proteins within this family range from 16 kD (DNAJC15) to 254 kD (DNAJC13). For this reason, a revised nomenclature was recently suggested (this issue of *Cell Stress and Chaperones*).

HSPA6 and HSPA7 were found only in humans while and although HSPA7 contains an internal frame shift and might be a pseudogene; bypassing the frame shift will result

in a protein with a full-length homology to HSPA1A. Thus, the HSPA7 protein with a full-length homology to HSPA1A might be produced, and this has recently been explained elsewhere (Broccieri et al. 2008).

Patterns of tissue specific HSPH, HSPA, and DNAJ expression

Cellular specialization may require specialized chaperone proteins and therefore may be responsible for part of the chaperone gene expansion. The expression pattern of most chaperone genes is currently unknown. An estimation of the expression pattern can be made by assessing the relative number of EST per tissue using the Unigene database (Schuler 1997). However, some caution should be taken as the Unigene assignments of ESTs to individual genes is not necessarily accurate (i.e., poor sequence quality and related sequences lead to incorrect 'binning' of some ESTs).

The expression estimates are displayed in Table 2 (HSPH/HSPA), Table 3 (DNAJA/B), and Table 4 (DNAJC). The peak expression for each tissue is indicated in bold. As expected, HSPA8 shows a high expression in most tissues (Table 2). In contrast, HSPH3, HSPA1L, HSPA6, HSPA7,

Table 2 Expression levels of HspH and HspA genes in various human tissues

	HSPH1	HSPH2	HSPH3	HSPH4	HSPA1A	HSPA1B	HSPAIL	HSPA2	HSPA5	HSPA6	HSPA7	HSPA8	HSPA9	HSPA12A	HSPA12B	HSPA13	HSPA14
Adipose tissue	152	76	0	76	684	608	0	0	608	76	0	989	76	76	0	0	76
Adrenal gland	180	120	0	210	1740	390	0	60	360	90	0	3780	510	90	0	90	30
Ascites	99	199	24	124	49	49	0	0	648	0	0	2720	923	0	0	24	24
Bladder	199	0	66	33	663	1161	0	0	199	99	33	1990	431	0	0	232	99
Blood	120	24	8	88	555	80	0	8	161	112	8	3069	386	0	0	40	40
Bone	125	153	0	97	153	0	0	0	501	13	27	1267	320	0	13	55	55
Bone marrow	142	61	0	447	40	81	0	40	610	20	0	1688	447	0	0	40	20
Brain	278	50	34	231	850	223	5	634	120	9	3	3672	338	87	8	130	67
Cervix	82	123	20	103	144	103	0	20	247	0	0	1257	453	0	20	103	82
Connective tissue	80	60	6	120	347	40	13	26	267	13	6	2145	227	26	0	60	26
Ear	183	61	0	0	734	0	0	122	122	0	0	367	61	61	0	0	0
Embryonic tissue	115	180	0	189	92	37	0	13	671	0	0	1315	278	13	0	83	92
Esophagus	246	98	49	689	2710	1724	0	246	1182	98	49	1921	542	0	0	49	197
Eye	61	109	23	85	180	56	14	42	185	14	14	1043	137	42	0	94	42
Heart	55	33	11	55	1638	365	11	66	188	33	11	2170	232	22	66	33	22
Intestine	127	131	4	233	1028	165	0	72	416	16	8	3552	271	4	4	33	29
Kidney	159	65	37	301	889	221	9	192	122	9	4	4628	348	56	42	94	18
Larynx	81	0	0	81	245	81	0	0	613	0	0	695	81	0	0	0	81
Liver	62	48	9	302	316	72	14	4	326	0	0	1238	273	0	0	33	33
Lung	124	97	23	198	1475	162	8	17	210	76	2	1174	239	0	17	50	20
Lymph	112	90	0	112	0	0	0	0	45	0	0	1373	315	0	0	0	0
Lymph node	185	108	0	10	0	10	0	0	174	0	0	566	152	0	0	87	217
Mammary gland	71	155	6	1237	589	97	25	12	719	12	6	2280	563	6	0	71	58
Mouth	295	191	29	280	1372	132	0	162	132	0	14	1918	575	0	0	29	103
Muscle	147	83	27	166	258	55	0	27	110	9	0	2949	342	27	0	27	27
Nerve	316	63	0	253	2658	253	0	0	379	0	63	1202	189	379	0	0	63
Ovary	38	87	0	136	58	87	0	0	428	19	0	1558	87	29	19	48	38
Pancreas	69	78	0	130	380	157	0	4	390	18	0	808	125	0	0	27	27
Parathyroid	48	0	48	0	0	0	0	0	48	0	0	484	436	48	0	0	339
Pharynx	0	48	0	48	24	0	0	24	96	0	0	2144	144	0	0	24	24
Pituitary gland	597	59	0	59	119	0	59	59	537	59	0	1732	179	119	0	0	59
Placenta	88	84	10	119	165	17	0	225	306	0	56	908	221	14	56	77	70
Prostate	41	115	15	120	1131	193	5	20	366	10	5	1560	146	20	0	36	47
Salivary gland	0	147	0	49	0	0	0	147	49	0	0	394	98	0	0	49	49
Skin	127	189	0	146	222	56	0	146	174	18	4	2622	411	18	9	14	47
Spleen	36	18	0	55	6992	1405	18	92	110	73	0	5512	295	18	110	18	18
Stomach	205	432	0	72	586	154	0	41	483	30	10	2038	123	0	10	0	20

Table 2 (continued)

	HSPH1	HSPH2	HSPH3	HSPH4	HSPA1A	HSPA1B	HSPA1L	HSPA2	HSPA5	HSPA6	HSPA7	HSPA8	HSPA9	HSPA12A	HSPA12B	HSPA13	HSPA14
Testis	365	93	223	374	193	42	105	543	262	0	3	2079	322	21	9	172	78
Thymus	135	36	12	110	1821	406	0	12	36	159	0	4270	258	0	12	49	61
Thyroid	166	41	20	229	500	312	20	0	1835	0	0	1335	584	104	20	0	62
Tonsil	58	117	0	58	58	0	0	58	0	0	0	469	0	0	0	0	234
Trachea	381	19	152	991	2345	801	0	57	38	190	57	3318	209	0	19	247	38
Umbilical cord	0	0	0	798	0	0	0	726	145	0	0	1597	145	0	72	0	0
Uterus	89	115	17	200	722	273	8	111	585	8	4	2381	290	21	8	81	34
Vascular	173	0	19	924	962	57	0	19	173	0	0	8356	423	38	0	115	0

Number of transcripts per million are indicated.

HSPA12A, and HSPA12B show very low levels in most tissues. HSPH3 and HSPA1L show the highest expression in the testis, which is in agreement with literature (Ito et al. 1998; Held et al. 2006). HSPA6 is absent under non-stress conditions and only expressed upon severe heat shock conditions (Noonan et al. 2007). The expression of HSPA1A is extremely variable, ranging from being absent in lymph (node), parathyroid, and umbilical cord to being expressed at very high levels in the spleen. As for the HSPH/HSPA family, the DNAJ family shows a highly variable expression profile (Tables 3 and 4). The highest expressed members throughout tissues are DNAJA1, DNAJB1, and DNAJB6 indicative of being “housekeeping” DNAJ chaperones although they all are lacking in a few tissues. As for the HSPA/HSPH families, the DNAJ family shows testis-specific members (DNAJB7, DNAJB8, DNAJC5B, and DNAJC5G). In general, with the exception of the testis, most HSP genes do not show an expression restricted to only a single tissue. In addition, peak levels per tissue are highly variable from gene to gene, providing no direct correlative clue for any specific partnerships between the diverse family members.

Patterns of developmental expression

We also used the Unigene database to look for developmental specific expression patterns (Table 5). The results show that HSPs are differentially expressed at different developmental stages. HSPA1A shows a large variation throughout different developmental stages. Interestingly, many DNAJC members are expressed during embryogenesis but are repressed in the neonate or infant (DNAC4-6 and DNAJC16-20). Only a minority of the genes were expressed the highest at adult stages.

Heat-induced transcription

Although HSPs were originally identified as heat inducible proteins, most members are identified according to presence of typical domains such as the HSP70 ATPase domain or the HSP40 DNAJ domain. For most of these members, it is currently unknown whether they are induced by heat. To investigate this, we used Affymetrix gene array data (Page et al. 2006) and performed a biased search on the heat inducibility for HSPH, HSPA, and DNAJ members (Table 6). We used an arbitrary threshold of twofold induction to define heat inducibility. Using this threshold, we found that HSPH1, HSPA1A, HSPA1B, HSPA1L, HSPA6, DNAJB1, DNAJB2, DNAJB4, and DNAJB6 are the major heat-inducible genes in HeLa cells. Thus, the majority of HSPs are not heat inducible. Of course, it must be noted that these patterns could be different for other cell lines and other heat conditions.

Table 3 Expression levels of DnaJA and DnaJB genes in various human tissues

	DNAJA1	DNAJA2	DNAJA3	DNAJA4	DNAJB1	DNAJB2	DNAJB4	DNAJB5	DNAJB6	DNAJB7	DNAJB8	DNAJB9	DNAJB11	DNAJB12	DNAJB13	DNAJB14
Adipose tissue	532	76	76	0	1065	76	152	0	152	0	0	76	0	152	0	76
Adrenal gland	180	60	30	0	210	0	30	60	180	0	0	0	0	120	0	30
Ascites	224	124	149	0	374	74	0	0	324	0	0	0	49	74	0	49
Bladder	165	66	66	99	199	66	99	0	132	0	0	33	0	33	0	0
Blood	169	96	88	32	128	24	32	8	161	0	0	32	56	32	0	32
Bone	125	194	69	0	125	83	27	27	125	0	0	27	41	27	0	0
Bone marrow	183	20	61	20	244	20	122	0	122	0	0	0	40	40	0	0
Brain	264	62	115	54	191	84	72	45	221	0	3	66	31	58	0	26
Cervix	268	20	82	82	164	20	20	0	82	0	0	41	82	20	0	0
Connective tissue	93	26	53	20	93	26	53	6	200	0	0	60	26	20	6	20
Ear	122	0	0	0	61	0	0	0	61	0	0	0	122	0	0	0
Embryonic tissue	305	46	55	0	120	41	32	37	236	0	0	18	74	27	0	50
Esophagus	98	98	246	49	246	49	344	0	344	0	0	0	0	147	0	0
Eye	208	52	23	42	227	94	23	42	170	4	0	33	66	33	0	37
Heart	143	44	33	88	265	22	166	55	199	0	0	99	121	66	0	0
Intestine	165	123	80	29	237	33	12	12	191	0	0	29	42	63	0	25
Kidney	202	23	47	14	197	42	117	32	225	0	0	117	18	84	0	18
Larynx	0	163	0	40	0	40	0	163	204	0	0	0	40	0	0	0
Liver	196	96	38	33	177	48	144	9	172	0	0	38	38	24	4	14
Lung	171	47	50	70	275	79	23	17	162	0	0	47	62	59	2	41
Lymph	90	22	90	0	67	90	22	0	157	0	0	0	112	22	0	0
Lymph node	76	43	32	54	76	32	0	10	76	10	0	10	32	65	0	152
Mammary gland	129	90	90	71	362	25	25	12	317	0	0	45	38	58	0	51
Mouth	29	88	118	88	88	44	14	0	354	0	0	29	14	29	0	14
Muscle	203	120	101	27	166	55	92	64	166	0	0	27	18	83	0	55
Nerve	189	0	126	189	696	189	189	0	63	0	0	63	63	126	0	0
Ovary	136	87	107	9	185	48	9	38	116	0	0	9	19	19	9	0
Pancreas	116	27	51	41	199	65	13	4	176	0	0	51	65	55	0	55
Parathyroid	0	0	0	48	145	0	0	48	48	0	0	0	48	96	0	0
Pharynx	578	48	48	24	120	0	0	0	506	0	0	24	24	72	0	96
Pituitary gland	478	59	0	119	298	119	59	59	179	0	0	59	0	0	0	59
Placenta	133	91	49	10	186	66	31	3	154	0	0	169	116	56	0	63
Prostate	99	62	52	26	235	52	10	57	115	0	0	47	104	68	10	20
Salivary gland	98	49	197	0	98	0	147	0	98	0	0	98	0	197	0	0
Skin	170	61	70	75	226	61	42	51	396	0	0	9	42	61	0	23
Spleen	129	92	55	18	591	18	0	18	295	0	0	55	55	55	0	36
Stomach	205	20	61	41	102	41	41	0	236	0	0	51	102	10	0	10

Table 3 (continued)

	DNAJA1	DNAJA2	DNAJA3	DNAJA4	DNAJB1	DNAJB2	DNAJB4	DNAJB5	DNAJB6	DNAJB7	DNAJB8	DNAJB9	DNAJB11	DNAJB12	DNAJB13	DNAJB14
Testis	277	114	63	51	546	30	24	18	253	24	39	87	27	48	15	15
Thymus	12	49	49	24	184	36	73	0	196	0	0	73	24	24	0	12
Thyroid	208	146	62	20	104	125	41	20	104	20	0	20	146	20	0	0
Tonsil	880	0	58	0	58	117	0	0	0	0	0	0	58	176	0	0
Trachea	190	57	19	247	228	19	19	0	152	0	0	114	0	19	38	19
Umbilical cord	72	0	0	0	0	0	0	0	0	0	0	0	0	145	0	0
Uterus	286	111	25	42	324	38	47	34	252	0	0	21	34	55	12	25
Vascular	481	38	38	0	211	0	423	0	288	0	0	77	0	19	0	0

Number of transcripts per million are indicated

Subcellular localization

Determination of HSP localization is essential to understand its biochemical function. Unfortunately, high-throughput analysis of HSP localization without the use of possible interfering tags is currently impossible due to the lack of specific antibodies. As subcellular localization signals share common characteristics, computational methods have been developed to predict the subcellular localization of proteins (Sprenger et al. 2006). We selected several publicly available localization prediction methods, which accept large batches of protein sequences and which were able to predict all of the major subcellular localizations. The selected methods were Wolf PSORT (Horton et al. 2007), pTarget (Guda 2006), CELLO (Yu et al. 2006), Multiloc (Hoglund et al. 2006) and Proteome Analyst (Szafron et al. 2004). In addition, we searched the human protein database (Mishra et al. 2006) for experimentally verified HSP localizations. As can be seen from Table 7, there are large variations in the prediction using the various programs. Therefore, we first searched for the prediction method that showed the highest accuracy for biochemical verified HSP members such as HSPA1A/HSP70 (cytosol/nucleus), HSPA1B/HSP72 (cytosol/nucleus), HSPA8/Hsc70 (cytosol/nucleus), HSPA5/Bip (ER), HSPA9/Grp75 (mitochondria), DNAJA3/Tid1 (Mitochondria), DNAJB1/HSP40 (cytosol/nucleus), DNAJB9/ERdj4 (ER) DNAJB11/ERdj3 (ER), DNAJC1/ERdj1 (ER), DNAJC10/ERdj5 (ER), and DNAJC19/TIM14 (mitochondria). Out of these 12 known localized proteins, the following number of correct predictions was found: Wolf PSORT: 7; pTarget: 10; CELLO: 8; Multiloc: 7; and Proteome Analyst: 10. Thus, Proteome Analyst and CELLO showed the highest correct prediction. However, it should be noted that at this stage, all prediction are potentially unreliable and should be used carefully. The scoring of the most reliable prediction method does rely on a relatively low number of verified chaperone proteins and the most reliable prediction program could therefore change in the future once more proteins will be experimentally verified.

We used the PrePS webserver to predict farnesylation of chaperones. As shown in Table 7, DNAJA1 and DNAJA4 are predicted to be prenylated by farnesyltransferase, which is in agreement with the literature (Terada and Mori 2000). In addition, DNAJB2b was predicted to be prenylated by geranylgeranyltransferase I as shown in the literature (Chapple and Cheetham 2003).

Homology of HSPH, HSPA, and DNAJ paralogs

Next, we computed protein similarity trees based on the alignments of the HSP protein sequences using the Neighboring-joining clustering method (Gascuel and Steel

Table 4 Expression levels of DnaJC genes in various human tissues

	DNAJC1	DNAJC2	DNAJC3	DNAJC4	DNAJC5	DNAJC5B	DNAJC5G	DNAJC6	DNAJC7	DNAJC8	DNAJC9
Adipose tissue	0	0	0	76	0	0	0	0	152	152	0
Adrenal gland	60	0	30	0	0	0	0	0	210	210	30
Ascites	24	74	0	24	49	0	0	0	249	199	24
Bladder	0	33	33	0	33	0	0	0	66	132	66
Blood	24	40	56	0	80	0	0	0	64	499	16
Bone	111	27	0	27	69	0	0	0	69	181	27
Bone marrow	0	20	40	40	0	0	0	20	81	183	20
Brain	16	15	18	21	64	4	1	231	84	54	17
Cervix	0	82	0	0	20	0	0	0	61	164	20
Connective tissue	66	0	6	46	53	6	0	0	33	233	33
Ear	61	0	0	0	0	0	0	0	0	61	122
Embryonic tissue	37	41	9	23	50	0	4	4	88	189	32
Esophagus	0	0	197	0	0	0	0	0	147	49	49
Eye	28	14	4	75	137	0	0	23	109	128	23
Heart	22	22	0	44	33	0	0	11	44	177	33
Intestine	84	29	16	93	123	0	0	12	67	131	72
Kidney	61	37	28	112	18	0	0	18	61	94	37
Larynx	122	40	0	122	81	0	0	0	0	0	0
Liver	72	95	14	0	38	0	0	4	62	134	19
Lung	65	32	17	133	109	2	0	14	59	174	50
Lymph	22	22	45	22	90	0	0	45	337	157	0
Lymph node	0	32	21	130	119	0	0	0	21	76	43
Mammary gland	25	58	19	45	116	12	0	6	97	64	19
Mouth	14	0	14	59	0	0	0	0	29	44	0
Muscle	0	0	36	18	110	0	0	18	18	83	0
Nerve	0	0	0	0	63	0	0	253	0	0	63
Ovary	29	38	9	87	77	0	0	0	38	224	19
Pancreas	37	4	4	55	74	0	0	9	46	65	4
Parathyroid	193	0	0	290	0	0	0	0	48	581	0
Pharynx	0	0	24	0	0	0	0	0	24	963	0
Pituitary gland	0	0	0	59	59	0	0	59	0	0	0
Placenta	49	17	31	21	17	10	0	42	66	151	7
Prostate	41	26	10	94	94	0	0	0	115	89	15
Salivary gland	0	0	0	0	0	0	0	0	147	0	0
Skin	66	47	14	28	85	0	0	14	56	160	42
Spleen	36	73	18	36	55	0	0	0	92	73	0
Stomach	41	30	10	30	82	0	0	10	113	123	10
Testis	18	72	21	66	30	45	39	9	57	81	6
Thymus	73	36	0	12	0	0	0	0	36	12	12
Thyroid	62	20	0	41	20	0	0	0	125	20	0
Tonsil	58	0	0	58	0	0	0	0	58	117	0
Trachea	38	76	114	0	19	0	0	0	57	38	0
Umbilical cord	290	0	72	0	0	0	0	0	145	0	0
Uterus	34	55	8	4	55	0	0	0	111	149	12
Vascular	19	19	57	0	19	0	0	19	115	57	0

2006). Figure 1 shows the output of these alignments depicted as phylograms. Three subfamilies can be derived from Fig. 1A. As expected, the first contains all the HSPH/HSP110 members. The second subfamily contains the cytosolic predicted HSPA proteins HSPA1A, HSPA1B, HSPA1L, HSPA2, HSPA6, and HSPA8 and is flanked by the ER-localized HSPA5 and the mitochondrial-localized HSPA9 protein. The third subfamily consists of the

distantly related HSPA12A and HSPA12B proteins. Thus, a high number of highly related HSPA proteins are localized in the cytosolic/nuclear compartment. To date, the reason for so many highly related cytosolic HSPA proteins is unknown.

DNAJ proteins can be divided in three subfamilies on the basis of the primary amino acid composition and are classified as type A, B and C proteins (Hennessy et al.

	DNAJC10	DNAJC11	DNAJC12	DNAJC13	DNAJC14	DNAJC15	DNAJC16	DNAJC17	DNAJC18	DNAJC19	DNAJC20
Adipose tissue	0	228	0	0	0	0	0	0	0	0	0
Adrenal gland	30	90	0	30	60	30	0	0	0	60	0
Ascites	49	124	74	24	349	24	49	0	24	0	24
Bladder	0	0	0	99	99	0	0	33	0	33	0
Blood	8	32	0	8	161	0	16	0	8	0	8
Bone	97	55	41	55	222	41	0	0	0	0	13
Bone marrow	61	20	122	20	40	0	61	0	0	101	0
Brain	73	114	19	31	58	40	15	20	119	70	3
Cervix	0	123	82	61	82	20	0	20	0	0	0
Connective tissue	100	33	106	113	200	167	13	6	20	6	6
Ear	183	0	0	0	0	61	0	0	0	61	0
Embryonic tissue	157	78	0	27	115	9	13	13	23	37	4
Esophagus	197	0	0	0	0	0	0	0	0	49	0
Eye	33	47	9	28	132	52	47	9	28	28	9
Heart	33	55	0	66	55	121	11	0	0	55	22
Intestine	38	59	16	25	67	72	50	0	0	127	12
Kidney	61	122	18	28	65	94	32	4	23	75	32
Larynx	0	0	0	40	163	0	0	40	0	0	0
Liver	148	24	24	24	100	28	9	14	0	19	4
Lung	65	65	20	17	168	29	35	14	5	32	26
Lymph	22	878	45	22	22	22	0	0	0	0	45
Lymph node	272	32	0	87	43	87	152	21	0	43	0
Mammary gland	90	90	19	32	155	38	0	25	6	51	0
Mouth	88	162	0	147	147	29	14	44	0	14	0
Muscle	46	147	18	27	92	36	36	18	46	92	0
Nerve	63	0	0	0	63	0	63	0	0	0	0
Ovary	29	48	0	38	107	0	29	0	9	9	0
Pancreas	102	32	69	18	69	46	4	0	0	27	4
Parathyroid	48	0	387	145	0	96	0	0	0	48	0
Pharynx	24	24	0	48	192	48	48	0	0	0	0
Pituitary gland	59	0	0	119	0	119	0	0	59	179	0
Placenta	38	59	0	42	98	42	31	24	7	35	7
Prostate	52	78	10	41	89	73	15	5	5	335	10
Salivary gland	0	0	197	98	49	0	0	49	0	147	0
Skin	70	66	9	103	151	33	4	4	4	28	14
Spleen	110	203	0	0	18	55	18	0	0	0	0
Stomach	82	51	0	41	41	30	0	51	10	0	0
Testis	338	141	12	60	162	39	33	6	147	33	3
Thymus	123	110	0	24	159	12	12	0	24	12	0
Thyroid	83	62	0	41	83	0	41	104	0	41	62
Tonsil	58	293	0	0	293	58	0	0	0	0	0
Trachea	648	133	0	57	38	19	38	38	0	19	0
Umbilical cord	217	0	0	0	0	0	0	0	0	0	0
Uterus	205	85	4	42	175	29	8	4	29	21	4
Vascular	269	19	0	115	38	77	0	0	0	96	0

2005). Type A proteins are the closest human orthologs of the *Escherichia coli* DNAJ and contain, besides an extreme N-terminal J-domain, a glycine/phenylalanine-rich region, a cysteine rich region, and a variable C-terminal domain. Type B proteins contain an N-terminal J-domain, a glycine/phenylalanine-rich region but lack the cysteine rich region. Type C DNAJ proteins contain only the J domain that is not necessarily restricted at the N-terminus but can be positioned at any place within the protein (Hennessy et al.

2005). The DNAJA is a highly related family of proteins and DNAJA3 (the mitochondrial localized member) is the most distantly related member (Fig. 1B). For the DNAJB family, three major subfamilies are found (Fig. 1C). The first consists of the members DNAJB2, DNAJB6, DNAJB7, and DNAJB8, the second of the members DNAJB1, DNAJB4, DNAJB5, DNAJB9, DNAJB11, and DNAJB13 and the third of the members DNAJB12 and DNAJB14. Although different C-termini could be defined

DNAJC21	DNAJC22	DNAJC23	DNAJC24	DNAJC25	DNAJC26	DNAJC27	DNAJC28	DNAJC29	DNAJC30
0	0	304	0	0	152	0	0	76	0
30	0	30	30	60	60	30	0	0	0
24	24	49	0	24	99	0	0	0	0
0	0	0	33	166	66	0	0	0	0
40	0	32	24	64	96	0	8	16	40
13	0	83	13	69	55	0	13	13	13
0	0	162	61	101	0	0	0	20	0
17	6	39	9	53	73	22	2	65	24
20	0	103	20	41	41	0	0	0	41
20	0	60	0	80	33	6	0	26	13
0	0	489	0	61	0	0	0	0	61
41	0	74	27	32	64	9	4	74	4
0	0	0	0	0	0	0	0	0	0
14	0	66	0	37	42	71	0	28	23
33	0	55	0	11	22	33	0	0	66
21	33	50	12	50	135	8	0	25	25
14	32	70	14	127	61	37	0	32	32
81	0	900	0	0	0	0	0	0	81
38	0	81	9	67	19	0	0	23	28
23	2	106	5	85	73	32	2	29	35
0	0	0	0	22	22	0	0	22	0
10	0	43	0	32	141	0	0	32	32
38	19	136	19	64	64	6	0	12	25
0	0	74	0	74	59	0	0	0	0
27	0	55	18	18	36	27	0	46	0
0	0	63	0	63	126	0	0	0	0
38	19	38	9	9	136	29	0	0	38
27	13	51	51	204	46	51	0	4	27
0	0	48	0	48	242	0	0	0	96
24	0	0	24	72	0	0	24	24	0
0	0	0	0	59	179	0	0	0	0
17	3	56	3	77	80	7	0	3	3
41	0	146	20	83	52	26	0	0	26
0	0	0	49	147	295	0	0	0	0
23	0	28	0	75	42	0	0	14	18
0	0	36	0	18	36	0	0	18	36
92	10	41	0	72	41	20	10	0	41
15	3	102	21	48	87	72	18	9	18
36	0	36	0	0	123	12	0	0	0
41	0	125	0	41	62	20	0	0	0
0	0	0	0	0	0	0	0	0	0
0	0	209	0	0	114	0	19	38	19
0	0	145	0	0	0	0	0	72	0
12	8	76	12	89	34	4	0	76	17
19	19	19	0	57	0	0	0	77	57

Number of transcripts per million are indicated

based on the primary amino acid level within the DNAJB family, at present, no clear biochemical function can be assigned to one of these subfamilies. The DNAJC family (Fig. 1D) shows the highest divergence of all families. Based on these results we decided to clone the HSPH, HSPA, DNAJA, and DNAJB family. As the DNAJC family is highly diverse, we omitted this family for library construction.

Cloning the HSPH, HSPA, and DNAJ gene families

Selection of an expression system

For cloning a human expression library to perform reverse genetic screens, we used a robust and versatile system with a high degree of flexibility: the Flp-In T-Rex tetracycline inducible expression system. The core promoter of this

Table 5 Expression levels of Hsp genes at various developmental stages

	Embryoid body	Blastocyst	Fetus	Neonate	Infant	Juvenile	Adult
HSPH1	254	32	165	160	168	394	127
HSPH2	98	208	61	0	42	89	132
HSPH3	0	0	15	0	42	0	13
HSPH4	254	224	181	224	0	538	185
HSPA1A	84	80	713	448	168	896	274
HSPA1B	70	32	155	128	42	215	105
HSPA1L	0	0	14	0	0	0	1
HSPA2	0	32	24	320	0	35	67
HSPA5	819	529	174	64	126	269	438
HSPA6	0	0	7	64	0	0	17
HSPA7	0	0	1	0	0	0	12
HSPA8	1102	1283	2208	6509	8999	7371	2014
HSPA9	339	288	211	577	337	789	265
HSPA12A	14	32	22	32	253	107	28
HSPA12B	0	0	8	64	0	0	13
HSPA13	84	96	77	0	84	0	54
HSPA14	56	64	52	0	253	35	52
DNAJA1	197	304	140	64	844	358	158
DNAJA2	56	80	51	64	84	89	86
DNAJA3	56	80	40	0	42	125	52
DNAJA4	0	0	75	0	0	53	45
DNAJB1	127	96	155	320	211	430	236
DNAJB2	42	48	47	0	0	53	77
DNAJB4	56	16	38	256	42	107	36
DNAJB5	28	80	82	0	168	0	24
DNAJB6	127	336	147	416	253	251	207
DNAJB7	0	0	3	0	0	17	0
DNAJB8	0	0	5	0	0	0	2
DNAJB9	28	0	22	0	126	89	57
DNAJB11	42	128	51	32	0	17	66
DNAJB12	42	16	33	64	42	0	51
DNAJB13	0	0	0	0	0	0	2
DNAJB14	42	48	26	64	42	17	38
DNAJC1	70	0	61	128	0	107	44
DNAJC2	56	64	33	32	42	17	35
DNAJC3	28	0	22	32	0	17	17
DNAJC4	28	0	58	0	0	0	46
DNAJC5	84	80	31	0	0	35	79
DNAJC5B	0	0	0	0	0	0	5
DNAJC5G	0	16	0	0	0	0	2
DNAJC6	14	0	58	0	0	71	27
DNAJC7	70	64	63	128	0	107	90
DNAJC8	127	192	105	160	84	161	131
DNAJC9	42	32	36	32	126	17	23
DNAJC10	240	144	73	160	84	358	72
DNAJC11	56	128	72	64	42	35	52
DNAJC12	0	0	40	0	0	0	30
DNAJC13	28	16	77	0	42	0	47
DNAJC14	155	160	81	32	0	35	115
DNAJC15	14	16	59	0	0	0	50
DNAJC16	0	16	12	0	0	53	26
DNAJC17	0	32	5	0	0	0	14
DNAJC18	14	64	118	0	42	0	16
DNAJC19	14	64	84	0	0	17	68

Table 5 (continued)

	Embryoid body	Blastocyst	Fetus	Neonate	Infant	Juvenile	Adult
DNAJC20	14	0	21	0	0	0	8
DNAJC21	70	48	36	32	0	0	35
DNAJC22	0	0	0	0	0	0	7
DNAJC23	70	80	81	64	0	143	94
DNAJC24	28	32	7	0	0	0	6
DNAJC25	56	16	56	64	0	0	67
DNAJC26	56	96	47	0	0	35	69
DNAJC27	0	16	51	0	0	0	13
DNAJC28	0	16	14	0	0	0	1
DNAJC29	70	112	75	64	0	17	14
DNAJC30	14	0	47	0	0	35	22

Number of transcripts per million

construct contains the full human cytomegalovirus (CMV) promoter followed by two tetracycline repressor binding sites. Thus, in cell systems engineered to express the tetracycline repressor, tetracycline can be used for regulated expression of the gene of interest, whereas full CMV strength promoter activity will be achieved in cell systems that do not contain the tetracycline repressor (Knopf et al. 2008). In addition to regulated expression, the vector contains an FRT recombination site for the FLP recombinase-mediated stable integration of the vector at a specific site in an engineered FRT site-harboring cell line (Garcia-Otin and Guillou 2006). The eukaryotic selection marker lacks a start codon, which selects for a site-specific integration in the target genome. We selected the FLP-In T-Rex 293 cell line, a modified human embryonic kidney (Hek-293) cell line that expresses the tetracycline repressor and harbors a single copy of the FRT site at an active site in the genome. The Hek-293 cell line has been used extensively as a model for protein-folding diseases and is widely known for its ease of manipulation (Graham et al. 1977). A summary of the FLP-In T-Rex system is depicted in Fig. 2.

Construction of vector fusion tags

Specific antibodies against most of the recently identified human heat shock proteins are not available. To verify the expression of the different proteins, we used a subset of frequently used protein tags. In some cases, protein tags interfere with the native function of the protein (Muller-Taubenberger 2006). Therefore, caution must be taken with the interpretation of the results obtained. In general, experiments using this library can always be confirmed using the non-tagged version. Although the protein expression cannot be confirmed with the untagged version, one

Table 6 Heat-induced transcription of hsp genes

Family	Gene Symbol	0.5 hour	2 hours	4 hours	Probe Set ID	
HSPH	HSPH1	0.9	2.6	3.1	206976_s_at	
	HSPH2	0.9	1.5	1.3	208814_at	
	HSPH3	0.9	1.8	2.0	205543_at	
	HSPH4	1.0	1.0	1.2	200825_s_at	
HSPA	HSPA1A	1.1	2.3	2.0	200799_at	
	HSPA1A /// HSPA1B	1.2	4.4	3.3	200800_s_at	
	HSPA1L	0.9	2.6	1.1	210189_at	
	HSPA2	0.9	1.0	0.9	211538_s_at	
	HSPA5	0.9	1.2	1.4	211936_at	
	HSPA6	1.3	64.1	5.8	117_at	
	HSPA8	0.9	1.1	0.9	208687_x_at	
	HSPA9B	0.9	0.9	1.0	200690_at	
	HSPA12A	0.9	0.8	0.7	214434_at	
	HSPA13	0.9	0.8	0.8	202557_at	
	HSPA14	1.0	0.9	0.9	219212_at	
	DNAJA	DNAJA1	1.0	1.5	1.5	200880_at
		DNAJA2	0.9	0.9	0.8	209157_at
		DNAJA3	0.9	0.9	0.7	205963_s_at
DNAJA4		1.1	1.9	1.2	220395_at	
DNAJB	DNAJB1	1.0	5.7	2.8	200664_s_at	
	DNAJB2	1.1	2.1	1.4	202500_at	
	DNAJB4	0.8	3.0	1.0	203810_at	
	DNAJB5	0.9	1.0	1.0	212817_at	
	DNAJB6	0.8	1.7	2.0	208810_at	
	DNAJB9	0.6	1.2	0.8	202843_at	
	DNAJB12	1.0	0.8	0.9	202865_at	
	DNAJB12	1.1	1.1	1.2	214338_at	
	DNAJB14	0.6	0.7	0.4	219237_s_at	
DNAJC	DNAJC1	1.3	1.0	1.1	218409_s_at	
	DNAJC3	1.0	0.8	1.0	208499_s_at	
	DNAJC4	1.0	1.0	1.1	206781_at	
	DNAJC6	0.8	0.7	0.7	204720_s_at	
	DNAJC7	1.0	1.2	1.4	202416_at	
	DNAJC8	0.8	0.8	0.9	212490_at	
	DNAJC9	0.9	0.9	1.0	213088_s_at	
	DNAJC10	0.9	0.8	0.8	221782_at	
	DNAJC11	1.0	0.9	1.0	215792_s_at	
	DNAJC12	1.0	0.8	0.8	218976_at	
	DNAJC13	1.0	0.9	0.8	212467_at	
	DNAJC15	1.0	1.0	1.0	218435_at	
	DNAJC16	0.7	0.8	0.5	212908_at	
	DNAJC17	1.1	1.0	1.2	219861_at	
	DNAJC22	1.0	1.0	1.0	216595_at	
DNAJC23	0.8	0.8	0.7	201914_s_at		
DNAJC26	1.1	1.0	1.1	202281_at		
DNAJC28	0.9	1.1	1.0	220372_at		
DNAJC29	1.0	0.6	0.7	213262_at		

Affymetrix gene array data.

Data are shown as fold change compared to an unheated control

can easily compare the biological effects detected in a particular assay.

As a first step toward a vector library for the expression of different heat shock proteins, we selected different protein tags harboring different biological properties. eGFP was selected for subcellular localization studies. As a second (smaller) tag, we used the V5 tag, consisting of only 14 amino acids for which high affinity antibodies are commercially available. In addition, we used a hexahistidine tag for protein precipitation experiments (Fig. 2).

To reduce cloning efforts, an N-terminal fusion tag was preferred. In this setting, we could maintain the natural stop codon in the gene of interest, which allows for simple shuttling from tagged to non-tagged constructs. However, it should be mentioned that N-terminal fusion tags could interfere with the import in subcellular organelles such as the ER or mitochondria and non-tagged versions are in such cases preferred.

An overview of the fusion tag cloning primers and procedure is shown in Fig. 2. The polymerase chain reaction (PCR) product of the eGFP gene lacking a stop-codon was cloned in pCDNA5/FRT/TO. For V5 and His tags, the corresponding oligos were annealed and cloned directly in the pCDNA5/FRT/TO vector.

Cloning the chaperone library

The focus of our gene library is on the cytosolic and nuclear expressed chaperones. Therefore, we selected the HSP70/HSPA proteins, which are putatively expressed in the cytosol or the nucleus (Table 7). For the HSP40/DNAJ family of proteins, we selected the major part of the DNAJA and DNAJB subfamily, which are the closest orthologs to *E. coli* DNAJ. As a certain human cell type typically only expresses a subset of its genes, we used pooled RNA from 10 different human cell lines as a source for cDNA synthesis and gene amplification. No amplification products were obtained for DNAJB4, DNAJB5, and DNAJB8. Instead, these genes were amplified from commercially obtained cDNA plasmids (Open Biosystems, Huntsville, AL). In addition, the HSPA6 gene was not amplified from the pooled cDNA. As this gene did not contain any introns, we amplified it directly from human chromosomal DNA. The yeast HSP70 gene SSA1 and the prokaryotic HSP70 gene DNAK were amplified from genomic *Saccharomyces cerevisiae* and *E. coli* DNA, respectively. An overview of the cloning procedure can be found in Fig. 2 and the cloning details can be found in Table 8. We used a nested PCR approach for the HSPH gene family as the start and the end of the members in this gene family are similar. The PCR products were purified, digested, and cloned in the pCDNA5/FRT/TO GFP vector. The constructs were sequence verified for the presence of

Table 7 Prediction of Hsp subcellular localization

		Wolf	Ptarget	Cello	Multiloc	Prot. analyst	Consensus	Experimental	Prenylation	
HSPH	HSPH1	c	c	c	c	c	c	–	No	
	HSPH2	c	c	n	c	c	c	g	No	
	HSPH3	c	c	n	n	c	c	c	No	
	HSPH4	e	m	c	e	e	e	e	No	
HSPA	HSPA1A	c	c	c	p	c	c	c	No	
	HSPA1B	c	c	c	p	c	c	c	No	
	HSPA1L	c	c	c	p	c	c	c	No	
	HSPA2	c	c	c	p	c	c	n	No	
	HSPA5	e	c	e	e	e	e	e	No	
	HSPA6	c	c	c	n	c	c	n	No	
	HSPA8	c	c	c	p	c	c	c	No	
	HSPA9	m	m	m	m	m	m	m	No	
	HSPA12A	m	–	m	m	–	m	–	No	
	HSPA12B	c	n	m	p	–	–	–	No	
	HSPA13	e	e	c	e	e	e	e	No	
	HSPA14	x	p	c	c	c	c	–	No	
	DNAJA	DNAJA1	c	c	n	c	e	c	c	Yes FT
		DNAJA2	c	c	n	n	e	cn	c	No
DNAJA3		m	m	m	m	m	m	m	No	
DNAJA4		c	c	n	c	e	c	a	Yes FT	
DNAJB	DNAJB1	n	n	c	c	c	c	c	No	
	DNAJB2a	n	n	c	c	–	cn	c	No	
	DNAJB2b	n	n	o	c	–	n	–	Yes FT GGT1	
	DNAJB4	c	c	c	c	e	c	–	No	
	DNAJB5	c	n	c	c	e	c	–	No	
	DNAJB6a	n	c	x	c	–	c	c	No	
	DNAJB6b	c	c	c	c	–	c	c	No	
	DNAJB7	n	c	o	n	–	n	–	No	
	DNAJB8	c	c	c	n	–	c	–	No	
	DNAJB9	x	e	c	x	c	xc	e	No	
	DNAJB11	x	e	c	e	e	e	e	No	
	DNAJB12	m	n	c	n	e	n	–	No	
	DNAJB13	c	c	c	c	c	c	–	No	
	DNAJB14a	c	c	c	n	e	c	–	No	
DNAJB14b	c	c	x	n	c	c	–	No		
DNAJC	DNAJC1	a	n	n	e	n	n	e	No	
	DNAJC2	n	–	n	n	n	n	–	No	
	DNAJC3	x	c	c	e	c	c	c	No	
	DNAJC4	c	n	n	n	c	n	–	No	
	DNAJC5	c	c	x	x	e	cx	v	No	
	DNAJC5B	c	c	x	a	e	c	–	No	
	DNAJC5G	c	n	x	c	e	c	–	No	
	DNAJC6	n	n	n	n	c	n	n	No	
	DNAJC7	n	c	n	c	c	c	c	No	
	DNAJC8	n	n	n	n	e	n	l	No	
	DNAJC9	c	e	c	c	–	c	–	No	
	DNAJC10	a	e	c	g	e	e	e	No	
	DNAJC11	c	c	n	n	–	cn	–	No	
	DNAJC12a	c	c	n	n	–	cn	–	No	
	DNAJC12b	c	c	n	c	–	c	–	No	
	DNAJC13	a	–	c	c	c	c	d	No	
	DNAJC14	c	n	m	n	e	n	e	No	
	DNAJC15	x	c	m	n	m	m	–	No	
DNAJC16	e	e	m	g	c	e	–	No		
DNAJC17	c	c	n	c	n	c	–	No		
DNAJC18	c	c	n	n	e	cn	–	No		

Table 7 (continued)

	Wolf	Ptarget	Cello	Multiloc	Prot. analyst	Consensus	Experimental	Prenylation
DNAJC19	x	m	m	m	m	m	m	No
DNAJC20	m	m	n	m	m	m	m	No
DNAJC21a	n	n	n	n	n	n	–	No
DNAJC21b	n	c	n	n	n	n	–	No
DNAJC22	a	e	a	y	ce	ae		no
DNAJC23	a	n	n	e	e	ne	e	No
DNAJC24	x	c	n	c	c	c	–	No
DNAJC25	a	c	a	e	c	ac	a	No
DNAJC26	a	m	n	n	c	n	c	No
DNAJC27	c	c	c	c	g	c	–	No
DNAJC28	m	m	m	m	–	m	–	No
DNAJC29	c	c	n	n	–	cn	–	No
DNAJC30	m	e	m	x	c	m	e	No

Legend: *n* nuclear, *m* mitochondrial, *g* Golgi, *e* er, *p* peroxisomes, *x* extracellular, *a* plasma membrane, *o* outer membrane, *v* cytoplasmic vesicle, *l* nucleolus, *d* endosome, *k* cytoskeleton, *y* lysosome, *FT* farnesyltransferase, *GGT1* geranylgeranyltransferase 1

the correct insert. Thereafter, expression was verified by Western blot analysis (data not shown) and the genes were subcloned in the pCDNA5/FRT/TO V5, pCDNA5/FRT/TO HIS, and the pCDNA5/FRT/TO vector.

Validation of the library

To test the effect of the different protein tags, two different biochemical assays were used. First, the effect of the tag on the ability of HSPA1A to assist the refolding of heat-denatured luciferase was tested (Michels et al. 1997, 1999). Therefore, we used constructs containing the HSPA1A gene downstream and in frame with the GFP tag, the V5 tag, and the pCDNA5/FRT/TO vector lacking a tag and compared the efficacy in the stimulation of luciferase refolding. The GFP tag significantly reduced the activity of the HSPA1A protein (Fig. 3A), whereas the V5 tag showed little to no significant effect on HSPA1A activity. Yet, modulation of HSPA1A related refolding by the co-factor BAG-1 (Nollen et al. 2000) could be achieved with all tagged versions (Fig. 3B). Thus, HSPA1A N-terminally tagged with eGFP may be less active related to non-tagged versions but seems unaffected in its ability to cooperate with its cofactors.

To test the effect of tagging DNAJ-like proteins, we used a filter trap assay to detect aggregation of polyglutamine proteins such as mutant Huntingtin. Aggregated Huntingtin is SDS-insoluble and retains trapped in a non-protein binding cellulose acetate membrane, and DNAJB1 is known to be able to inhibit this aggregation (Carra et al. 2005; Rujano et al. 2007). We used constructs containing

the DNAJB1 gene downstream and in frame with the GFP tag, the V5 tag, and the pCDNA5/FRT/TO vector lacking a tag and compared the efficacy of DNAJB1 in the suppression of mutant Huntingtin aggregation. As shown in Fig. 3C, untagged DNAJB1 strongly suppresses mutant Huntingtin aggregation containing a polyQ tract of 74 residues. Both the V5- and the GFP-tagged showed an equal slight reduction on the aggregation suppression but yet retained substantial activity. Thus, N-terminal tagging sometimes does influence the maximal activity of the chaperones tested. This implies that after performing experiments with our tagged HSPs, confirmation with untagged versions is required.

Conclusion/Discussion

The HSPH/HSPA and DNAJ families are large gene families with many poorly studied individual members. We used bioinformatics approaches to study the expression, the localization, and the homology of these families. These approaches generated large datasets, which will be useful for the systematic biochemical analysis of these family members. It was found that HSPs are expressed at highly variable levels in different tissues. So far, no clear patterns were seen for paired expression of certain members within, e.g., the HSPA and DNAJ family in most tissues. Although it is valid to search for the highest expressing tissue for a particular transcript, it is difficult to compare the level of different transcripts for a particular tissue. This is thought to be partly because different messengers show a different

Table 8 Summary of the library cloning

Family	Gene	5'-oligo	3'-oligo	Site 1	Site 2
HSP110	HSPH1	CTCCAGGGTTTCTTATCAG	GATTTAATCACAGCCCTCTTG	NA	NA
	HSPH1*	CACAGATACACCATGTCGGTGGGGTTG	CGGATCTCGAGCTAGTCCAAAGTCCATATAACAG	EcoRV	XhoI
	HSPH2	ACCCACTGGAAGGACTTAGG	GAGCTCTGGCATGTAAGTC	NA	NA
	HSPH2*	GACAGATATCACCATGTCGGTGGTGGGCATAGAC	GACTGGGGCCGGAAATCAATCAATGTCATTTCCAG	EcoRV	NorI
	HSPH3	GCAATAGCCCAAGAAAGGAC	GATGGACCCGTGGTTACTTG	NA	NA
	HSPH3*	GACGGATATCACCATGTCGTGGTGGCATTGAC	GATCGGGCCGAGACTTAGTCCACTTCCATCTC	EcoRV	NorI
	HSPA1A	ACCAGAGGATCCACCATGGCCAAAAGCCCGGGCAT	ATCACATGCGCCGCTTAATCACTACCTCTCTCAATGG	BamHI	NorI
	HSPA1L	CACAGATATCACCATGGTACTGCGCAAGGAAT	GACTGGGGCCGTTAATCTACTTCTTCAATGTGGGGC	EcoRV	NorI
	HSPA2	CACACAGGATCCACCATGTCTGCCGTGGCCCGCT	GACTGGGGCCGTTAGTCCACTTCTTCGATGGTGG	BamHI	NorI
	HSPA6	GACAGATATCACCATGCAGGCCCCACGGGAGCT	GACTGGGGCCGCTCAATCAACCTCTCTCAATGA	EcoRV	No I
HSP70	HSPA8	CACACAGGATCCACCATGTCCAAGGGACCTGCAGTTG	GACTGGGGCCGCTTAATCAACCTCTCTCAATGGTGGG	BamHI	NorI
	HSPA14	CACACAGGATCCACCATGGCCCATCGGAGTTCA	GACTGGGGCCGCTTAAAGATGCTATCTCAATAGAGATTG	BamHI	NorI
	DNAK	ACCAATGGATCCACCATGGGTAAATAATTTGGTATC	AATAATGGGGCCGCCCTGTGCAAGTATAATTAAC	BamHI	NorI
	SSA1	TACTAAGGATCCACCATGTCAAAAGCTGTGGTATTG	TAGTATGGGGCCGCTTAAATCAACTTCTTCAACGGTTGGACC	BamHI	NorI
	DNAJ1	CACAATGGATCCACCATGGTGAAGAACAACCTTACTACG	GACTGGGGCCGCTTAAAGAAGTCTGACACTGAAC	BamHI	NorI
	DNAJ2	ATCCACGGATCCACCATGGTAACTGGCTGACACG	GACTGGGGCCGCTTACTGATGGGCACACTGCAC	BamHI	NorI
	DNAJ3	ATTCGAGGATCCACCATGGCTGCGGGTGTCTCCACA	GACTGGGGCCGCTGATGGGATATCATGAGGTA	BamHI	NorI
	DNAJ4	ATAGCTGGATCCACCATGGTGAAGGAGACCCAGTA	GACTGGGGCCGCTCATGCCGTCTGGCCTGCAC	BamHI	NorI
	DNAJ1	CACAATGGATCCACCATGGTAAAGACTACTACCAGACG	GACTGGGGCCGCTATAITGGAAAGAACCTGCTCAAG	BamHI	NorI
	DNAJ2a	ATCGATGGATCCACCATGGCATCTTACTACGAGATC	TACGATGGGGCCGCTCAGAACAACATCTGCGGGTTTC	BamHI	NorI
DNAJ2b	ATCGATGGATCCACCATGGCATCTTACTACGAGATC	TACGATGGGGCCGCTCAGAGGATGAGGCAGCGAG	BamHI	NorI	
DNAJ3	TACTACGGATCCACCATGGTGGACTACTACGAGGT	TACTGTGGGGCCGCTTACTGAGTATTGATGCCAAGCAG	BamHI	NorI	
DNAJ4	TGCAAAGGATCCACCATGGGAAAGACTATTATTGC	GACTGGGGCCGCTATGAGGCAGGAAGATGTTCC	BamHI	NorI	
DNAJ5	GATCGGGCCGCACCATGGGAAAAGATTATACAAGATTCTTGGG	GATATCGGGCCCTAGGAACAAGGATAGGTCTGC	NorI	ApaI	
DNAJ6b	GATATAGGATCCACCATGGTGGATTAATGAAAGTTCT	GATATTGGGGCCGCTTACTTGTATCCAAGCGCAG	BamHI	NorI	
DNAJ6a	TATATAGGATCCACCATGGTGGATTAATGAAAGTTCT	TATATAGGGCCGCTTAGTGAITGCCITTTGGTCCG	BamHI	NorI	
DNAJ7	GATTACGATATCACCATGGTGGATTAATGAAAGT	GATTACGGGGCCGCTTAAACAATCTCTTTTGGTAGACTTC	EcoRV	NorI	
DNAJ8	AAGTAAGGATCCACCATGGCTAACTACTACGAAAGTG	GATATAGGGCCGCTTACTTGTCTGTCATCCATTTG	BamHI	NorI	
DNAJ9	GATCGGGCCGCACCATGGCTACTCCCCAGTCAAT	GATATCGGGCCCTACTGTCTGAAACAGTCAAG	NorI	ApaI	
DNAJ10	ATCGATGGATCCACCATGGCATCTTACTACGAGATTC	TACGATGGGGCCGCTCAGAACAACATCTGCTGGCTTC	BamHI	NorI	

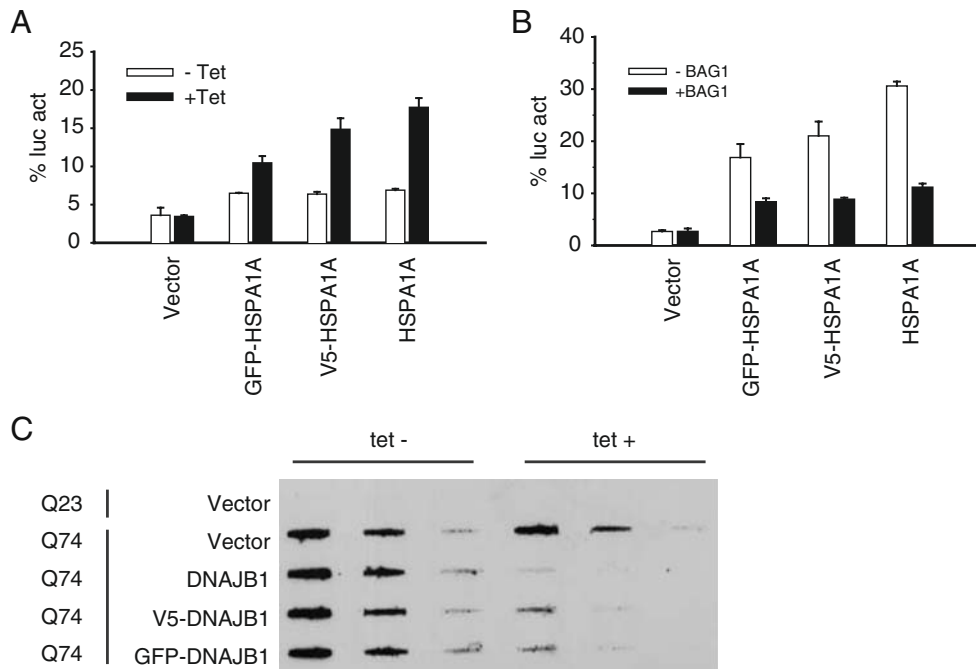


Fig. 3 The effect of different fusion tags on HSPA1A (A) and (B) or DNAJB1 (C). (A) Luciferase refolding assay using GFP, V5, and untagged HSPA1A versions. Cells were transfected with different tagged versions of HSPA1A together with a plasmid encoding firefly luciferase. HSPA1A expression was induced using tetracycline. The day after transfection, the cells were heated at 37°C or 45°C for 30 min and reincubated for 1 h at 37°C to allow luciferase refolding. Thereafter, cells were lysed and measured for luciferase activity. The percentage of luciferase activity is plotted relative to the activity in unheated control cells (100%). (B) Modulation of tagged HSPA1A versions by BAG-1. Cells were treated as in (A) but also co-transfected

with a BAG-1 encoding plasmid as indicated. (C) Filter trap assay showing aggregation of expanded Huntingtin. GFP, V5 and untagged versions of DNAJB1 were used as indicated. Cells were transfected with different tagged versions of DNAJB1 together with a plasmid encoding GFP-tagged Huntingtin containing either 23Q or 74Q. DNAJB1 was induced by tetracycline. Two days after transfection, cells were lysed and the lysates were loaded on to a cellulose acetate membrane. After transblotting, blots were immunostained for GFP to detect aggregated Huntingtin. GFP-tagged DNAJB1 alone did not show any signal on the membrane (not shown)

half-life and partly because different transcripts show large differences in the window of bottom-to-peak expression making such a comparison difficult. Interestingly, we did find some pattern for the testis. A testis-specific HSPA transcript was found (HSPA1L) as well as testis-specific DNAJ members (DNAJB7, DNAJB8, DNAJC5B, and DNAJC5G). This could indicate that HSPA1L cooperates with one of these DNAJ members.

We also studied the expression levels of HSPs during various developmental stages. The results of the peak expression per transcript show that there is a wide variation in HSP expression throughout different developmental stages but many DNAJC members peak at the blastocyst and fetal stages, indicating that there is a need for specialized DNAJ members early in development.

Surprisingly, the heat inducibility of the different HSPs was restricted to only a couple of members within each family (HSPH1, HSPA1A/B, HSPA6, DNAJB1, DNAJB2, DNAJB4, and DNAJB6). This could mean that HSPA1A or HSPA6 cooperate with HSPH1 and one of these DNAJ members following stress conditions. Interestingly, no heat-inducible DNAJC member was found indicating that

DNAJC members do not function in the stress response. It should be noted, however, that the array did not contain probes corresponding to all DNAJC members.

Analyzing the cellular distribution and homology of different HSP members showed that a very homologous subfamily of the HSPA family is predicted to be expressed in the cytosol (HSPA1A/B, HSPA1L, HSPA2, HSPA6, and HSPA8). This indicates that only a minority of the gene duplication occurred as a result of the compartmentalization. It is unclear at this stage if this homologous subgroup of HSPA chaperones is regulated by the same subset of co-factors and if they bind the same subset of client proteins. It will be highly interesting to answer these questions by using available biochemical approaches. For this purpose, we cloned a large collection of chaperone-encoded genes in a tetracycline-inducible vector system. Different tags with different properties were used in order to detect expression levels (V5), study subcellular localization in living or fixed cells (GFP/V5), or to enrich the expressed protein from crude cell lysates (His). In addition, non-tagged versions were made to verify obtained biological effects. This expression library will be useful to systematically study the biochemical

and cell biological features of these poorly characterized HSPs and might help answer the intriguing question why we have so many HSPA and DNAJ chaperones.

Acknowledgements We would like to thank Maria A.W.H. van Waarde for expert assistance on biochemical analysis. We thank Eefje Pelster, Alette H. Faber, and Reinier Bron for assistance on gene cloning. Lenja Bystriykh (Department of Cell Biology, Stem Cell Biology Section, University Medical Center Groningen, The Netherlands) is kindly acknowledged for help on the Unigene EST collection and Ron Dirks (section Biochemistry, Radboud University, Nijmegen, The Netherlands) for help on the Affimetrix gene array data. Russell S. Thomas (CIIT Centers for Health Research, NC, USA) is acknowledged for providing the array data sets. This work was supported by Innovatiegerichte Onderzoeksprogramma Genomics Grant IGE03018.

References

- Albanese V, Yam AY, Baughman J, Parnot C, Frydman J (2006) Systems analyses reveal two chaperone networks with distinct functions in eukaryotic cells. *Cell* 124:75–88 doi:10.1016/j.cell.2005.11.039
- Brocchieri L, Conway de ME, Macario AJ (2007) Chaperonomics, a new tool to study ageing and associated diseases. *Mech Ageing Dev* 128:125–136 doi:10.1016/j.mad.2006.11.019
- Brocchieri L, Conway de ME, Macario AJ (2008) HSP70 genes in the human genome: conservation and differentiation patterns predict a wide array of overlapping and specialized functions. *BMC Evol Biol* 8:19 doi:10.1186/1471-2148-8-19
- Carra S, Sivilotti M, Chavez Zobel AT, Lambert H, Landry J (2005) HSPB8, a small heat shock protein mutated in human neuromuscular disorders, has in vivo chaperone activity in cultured cells. *Hum Mol Genet* 14:1659–1669 doi:10.1093/hmg/ddi174
- Chapple JP, Cheetham ME (2003) The chaperone environment at the cytoplasmic face of the endoplasmic reticulum can modulate rhodopsin processing and inclusion formation. *J Biol Chem* 278:19087–19094 doi:10.1074/jbc.M212349200
- Garcia-Otin AL, Guillou F (2006) Mammalian genome targeting using site-specific recombinases. *Front Biosci* 11:1108–1136 doi:10.2741/1867
- Gascuel O, Steel M (2006) Neighbor-joining revealed. *Mol Biol Evol* 23:1997–2000 doi:10.1093/molbev/msl072
- Graham FL, Smiley J, Russell WC, Nairn R (1977) Characteristics of a human cell line transformed by DNA from human adenovirus type 5. *J Gen Virol* 36:59–74 doi:10.1099/0022-1317-36-1-59
- Gribaldo S, Lumia V, Creti R, de Macario EC, Sanangelantoni A, Cammarano P (1999) Discontinuous occurrence of the HSP70 (dnaK) gene among Archaea and sequence features of HSP70 suggest a novel outlook on phylogenies inferred from this protein. *J Bacteriol* 181:434–443
- Guda C (2006) pTARGET: a web server for predicting protein subcellular localization. *Nucleic Acids Res* 34:W210–W213 doi:10.1093/nar/gkl093
- Hageman J, Eggen BJ, Rozema T, Damman K, Kampinga HH, Coppes RP (2005) Radiation and transforming growth factor-beta cooperate in transcriptional activation of the profibrotic plasminogen activator inhibitor-1 gene. *Clin Cancer Res* 11:5956–5964 doi:10.1158/1078-0432.CCR-05-0427
- Held T, Paprotta I, Khulan J et al (2006) HSPA4I-deficient mice display increased incidence of male infertility and hydronephrosis development. *Mol Cell Biol* 26:8099–8108 doi:10.1128/MCB.01332-06
- Hennessy F, Nicoll WS, Zimmermann R, Cheetham ME, Blatch GL (2005) Not all J domains are created equal: implications for the specificity of HSP40–HSP70 interactions. *Protein Sci* 14:1697–1709 doi:10.1110/ps.051406805
- Hoglund A, Donnes P, Blum T, Adolph HW, Kohlbacher O (2006) MultiLoc: prediction of protein subcellular localization using N-terminal targeting sequences, sequence motifs and amino acid composition. *Bioinformatics* 22:1158–1165 doi:10.1093/bioinformatics/btl002
- Horton P, Park KJ, Obayashi T, Fujita N, Harada H, Adams-Collier CJ, Nakai K (2007) WoLF PSORT: protein localization predictor. *Nucleic Acids Res* 35:W585–W587 doi:10.1093/nar/gkm259
- Ito Y, Ando A, Ando H, Ando J, Saijoh Y, Inoko H, Fujimoto H (1998) Genomic structure of the spermatid-specific HSP70 homolog gene located in the class III region of the major histocompatibility complex of mouse and man. *J Biochem* 124:347–353
- Kampinga HH (2006) Chaperones in preventing protein denaturation in living cells and protecting against cellular stress. *Handb Exp Pharmacol* 172:1–42
- Knopf CW, Zavidij O, Rezuchova I, Rajcani J (2008) Evaluation of the T-REX transcription switch for conditional expression and regulation of HSV-1 vectors. *Virus Genes* 36:55–66 doi:10.1007/s11262-007-0178-9
- Larkin MA, Blackshields G, Brown NP et al (2007) Clustal W and Clustal X version 2.0. *Bioinformatics* 23:2947–2948 doi:10.1093/bioinformatics/btm404
- Maglott D, Ostell J, Pruitt KD, Tatusova T (2007) Entrez gene: centered information at NCBI. *Nucleic Acids Res* 35:D26–D31 doi:10.1093/nar/gkl993
- Maurer-Stroh S, Koranda M, Benetka W, Schneider G, Sirota FL, Eisenhaber F (2007) Towards complete sets of farnesylated and geranylgeranylated proteins. *PLoS Comput Biol* 3:e66 doi:10.1371/journal.pcbi.0030066
- Michels AA, Nguyen VT, Konings AW, Kampinga HH, Bensaude O (1995) Thermostability of a nuclear-targeted luciferase expressed in mammalian cells. Destabilizing influence of the intranuclear microenvironment. *Eur J Biochem* 234:382–389 doi:10.1111/j.1432-1033.1995.382_b.x
- Michels AA, Kanon B, Konings AW, Ohtsuka K, Bensaude O, Kampinga HH (1997) HSP70 and HSP40 chaperone activities in the cytoplasm and the nucleus of mammalian cells. *J Biol Chem* 272:33283–33289 doi:10.1074/jbc.272.52.33283
- Michels AA, Kanon B, Bensaude O, Kampinga HH (1999) Heat shock protein (HSP) 40 mutants inhibit HSP70 in mammalian cells. *J Biol Chem* 274:36757–36763 doi:10.1074/jbc.274.51.36757
- Mishra GR, Suresh M, Kumaran K et al (2006) Human protein reference database – 2006 update. *Nucleic Acids Res* 34:D411–D414 doi:10.1093/nar/gkj141
- Muller-Taubenberger A (2006) Application of fluorescent protein tags as reporters in live-cell imaging studies. *Methods Mol Biol* 346:229–246
- Nollen EA, Brunsting JF, Song J, Kampinga HH, Morimoto RI (2000) Bag1 functions in vivo as a negative regulator of HSP70 chaperone activity. *Mol Cell Biol* 20:1083–1088 doi:10.1128/MCB.20.3.1083-1088.2000
- Noonan EJ, Place RF, Giardina C, Hightower LE (2007) HSP70B' regulation and function. *Cell Stress Chaperones* 12:219–229 doi:10.1379/CSC-278.1
- Page RD (1996) TreeView: an application to display phylogenetic trees on personal computers. *Comput Appl Biosci* 12:357–358
- Page TJ, Sikder D, Yang L, Pluta L, Wolfinger RD, Kodadek T, Thomas RS (2006) Genome-wide analysis of human HSF1 signaling reveals a transcriptional program linked to cellular adaptation and survival. *Mol Biosyst* 2:627–639 doi:10.1039/b606129j

- Rudiger S, Germeroth L, Schneider-Mergener J, Bukau B (1997) Substrate specificity of the DnaK chaperone determined by screening cellulose-bound peptide libraries. *EMBO J* 16:1501–1507 doi:[10.1093/emboj/16.7.1501](https://doi.org/10.1093/emboj/16.7.1501)
- Rudiger S, Schneider-Mergener J, Bukau B (2001) Its substrate specificity characterizes the DNAJ co-chaperone as a scanning factor for the DnaK chaperone. *EMBO J* 20:1042–1050 doi:[10.1093/emboj/20.5.1042](https://doi.org/10.1093/emboj/20.5.1042)
- Rujano MA, Kampinga HH, Salomons FA (2007) Modulation of polyglutamine inclusion formation by the HSP70 chaperone machine. *Exp Cell Res* 313:3568–3578 doi:[10.1016/j.yexcr.2007.07.034](https://doi.org/10.1016/j.yexcr.2007.07.034)
- Sahi C, Craig EA (2007) Network of general and specialty J protein chaperones of the yeast cytosol. *Proc Natl Acad Sci U S A* 104:7163–7168 doi:[10.1073/pnas.0702357104](https://doi.org/10.1073/pnas.0702357104)
- Schuler GD (1997) Pieces of the puzzle: expressed sequence tags and the catalog of human genes. *J Mol Med* 75:694–698 doi:[10.1007/s001090050155](https://doi.org/10.1007/s001090050155)
- Sprenger J, Fink JL, Teasdale RD (2006) Evaluation and comparison of mammalian subcellular localization prediction methods. *BMC Bioinformatics* 7(Suppl 5):S3 doi:[10.1186/1471-2105-7-S5-S3](https://doi.org/10.1186/1471-2105-7-S5-S3)
- Szafron D, Lu P, Greiner R et al (2004) Proteome Analyst: custom predictions with explanations in a web-based tool for high-throughput proteome annotations. *Nucleic Acids Res* 32:W365–W371 doi:[10.1093/nar/gkh485](https://doi.org/10.1093/nar/gkh485)
- Terada K, Mori M (2000) Human DNAJ homologs dj2 and dj3, and bag-1 are positive cochaperones of hsc70. *J Biol Chem* 275:24728–24734 doi:[10.1074/jbc.M002021200](https://doi.org/10.1074/jbc.M002021200)
- Wheeler DL, Barrett T, Benson DA et al (2007) Database resources of the National Center for Biotechnology Information. *Nucleic Acids Res* 35:D5–D12 doi:[10.1093/nar/gkl1031](https://doi.org/10.1093/nar/gkl1031)
- Yu CS, Chen YC, Lu CH, Hwang JK (2006) Prediction of protein subcellular localization. *Proteins* 64:643–651 doi:[10.1002/prot.21018](https://doi.org/10.1002/prot.21018)